JOURNAL OF BACTERIOLOGY, Feb. 2008, p. 1036–1044 Vol. 190, No. 3
0021-9193/08/$08.00+0 doi:10.1128/JB.01416-07

Identification and Characterization of an *Acinetobacter baumannii* Biofilm-Associated Protein▽

Thomas W. Loehfelm,[1,3] Nicole R. Luke,[1,4] and Anthony A. Campagnari[1,2,3,4]*

Department of Microbiology and Immunology[1] and Department of Medicine, Division of Infectious Diseases,[2] and Witebsky Center for Microbial Pathogenesis and Immunology,[3] University at Buffalo, The State University of New York, and NYS Center of Excellence in Bioinformatics and Life Sciences,[4] Buffalo, New York

Received 31 August 2007/Accepted 7 November 2007

We have identified a homologue to the staphylococcal biofilm-associated protein (Bap) in a bloodstream isolate of *Acinetobacter baumannii*. The fully sequenced open reading frame is 25,863 bp and encodes a protein with a predicted molecular mass of 854 kDa. Analysis of the nucleotide sequence reveals a repetitive structure consistent with bacterial cell surface adhesins. Bap-specific monoclonal antibody (MAb) 6E3 was generated to an epitope conserved among 41% of *A. baumannii* strains isolated during a recent outbreak in the U.S. military health care system. Flow cytometry confirms that the MAb 6E3 epitope is surface exposed. Random transposon mutagenesis was used to generate *A. baumannii bap1302*::EZ-Tn*5*, a mutant negative for surface reactivity to MAb 6E3 in which the transposon disrupts the coding sequence of *bap*. Time course confocal laser scanning microscopy and three-dimensional image analysis of actively growing biofilms demonstrates that this mutant is unable to sustain biofilm thickness and volume, suggesting a role for Bap in supporting the development of the mature biofilm structure. This is the first identification of a specific cell surface protein directly involved in biofilm formation by *A. baumannii* and suggests that Bap is involved in intercellular adhesion within the mature biofilm.

Acinetobacter spp. are gram-negative aerobic coccobacilli that are ubiquitous in nature, persistent in the hospital environment, and cause a variety of opportunistic nosocomial infections (1). A number of species of *Acinetobacter* are associated with human infection, including genomic species 3 and 13TU (8, 46), although *A. baumannii* is generally regarded as the major pathogen. *A. baumannii* is a causative agent of nosocomial pneumonia, bacteremia, meningitis, and urinary tract infection (1) and more recently has caused serious infections among American military personnel serving in Iraq and Afghanistan (12, 38). Because it is often multi- or pan-drug resistant, infections are difficult to treat (17), resulting in attributable mortalities of up to 23% for hospitalized patients and 43% for patients under intensive care (16). Indeed, the Antimicrobial Availability Task Force of the Infectious Diseases Society of America recently identified *A. baumannii*, along with *Aspergillus* spp., extended-spectrum β-lactamase-producing *Enterobacteriaceae*, vancomycin-resistant *Enterococcus faecium*, *Pseudomonas aeruginosa*, and methicillin-resistant *Staphylococcus aureus*, as "particularly problematic pathogens" for which there is a desperate need for new drug development (42). In the case of *A. baumannii*, there is an additional unmet need for an understanding of its basic pathogenesis.

Most *A. baumannii* research to date has focused on cataloging and understanding the variety of antimicrobial resistance genes and mechanisms found within the species (3, 30, 45, 50). An intriguing observation that ethanol stimulates the virulence of *A. baumannii* (39) led to the identification of a number of genes affecting virulence toward *Caenorhabditis elegans* and *Dictyostelium discoideum* (40) that await further characterization. A well-characterized porin of *A. baumannii*, the 38-kDa outer membrane protein A, has been shown to induce apoptosis of eukaryotic cells (9) and to activate dendritic cells, leading to the differentiation of $CD4^+$ T cells toward a Th1 phenotype (26). Finally, it was noted that *A. baumannii* forms biofilms with enhanced antibiotic resistance (48, 49) and, more recently, that a chaperone-usher secretion system involved in pilus assembly affects biofilm formation (44).

Biofilms are highly structured communities of bacteria attached to a surface (41) and are recognized as a common cause of human infection (10). It has been proposed that all bacterial biofilms have a number of functionally conserved components in common, including the production of an extracellular polysaccharide matrix, GGDEF/EAL-domain-mediated intracellular signaling, and large surface adhesins homologous to the biofilm-associated protein (Bap) first identified in *S. aureus* (23). Bap family members are defined as high-molecular-weight proteins that are present on the bacterial surface, contain a core domain of tandem repeats, and confer on bacteria the ability to form a biofilm (24). Since the initial identification of Bap, homologues have been identified in at least 13 pathogenic species (24, 25), and the proteins generally share structural and functional similarities, although not necessarily primary sequence similarity.

In the present study, we have identified and fully sequenced a gene encoding a Bap homologue in *A. baumannii* 307-0294. We have generated a transposon-insertion mutant deficient in Bap surface expression and a specific monoclonal antibody (MAb), 6E3, recognizing Bap. The epitope recognized by MAb 6E3 is surface accessible and conserved among 41% of *A.*

* Corresponding author. Mailing address: Department of Microbiology and Immunology, University at Buffalo, Rm. 140, Biomedical Research Building, 3435 Main St., Buffalo, NY 14214. Phone: (716) 829-2673. Fax: (716) 829-3889. E-mail: aac@buffalo.edu.

▽ Published ahead of print on 16 November 2007.

TABLE 1. Sequences of oligonucleotide primers used for RT-PCR

Primer	Sequence (5′–3′)	Position[a]	Target
1124	TCATACGTCTGAAA AATGGCGAG	152–174	5′ region of *bap*
1125	CATCAAGTGCTACT GTCGGCG	1151–1171(c)	5′ region of *bap*
1461	CAGATGTGCCTCAT TTGTCGG	25025–25045	3′ region of *bap*
1462	CCTGTATTCACTCC TTGACCAGCAG	25259–25283(c)	3′ region of *bap*
1160	AAGGAGTGAATAC AGGCGAAG	25268–25288	3′ *bap* to A1S_2695
1330	CATTTGCATCGTAG CGACTCG	26572–26592(c)	3′ *bap* to A1S_2695
1437	ACCAAATAGAGCA GCAGGTTC	26278–26298	A1S_2695
1438	CTCCCCTTCTTTACC ATCAATC	26888–26909(c)	A1S_2695

[a] That is, relative to the predicted *bap* start codon. The predicted *bap* coding sequence is from positions 1 to 25863, and that of A1S_2695 is from positions 26160 to 27665. The "(c)" indicates that the primer anneals to the cDNA strand.

baumannii isolates recovered during the U.S. military health care system outbreak. Quantitative comparison of biofilms formed by a Bap-deficient mutant and wild-type bacteria demonstrates that the mutant is unable to sustain biovolume and biofilm thickness development.

MATERIALS AND METHODS

Bacterial strains and culture conditions. Wild-type *A. baumannii* strain 307-0294 was isolated from the bloodstream of a patient in 1994. A library of 98 *Acinetobacter* strains was obtained from the Walter Reed Army Medical Center, including 76 isolates of *A. baumannii*, 13 isolates of genome species 3, 5 isolates of species 13TU, 1 isolate of genome species 10, and 3 isolates of otherwise-uncharacterized *Acinetobacter* sp. *Escherichia coli* XL1-Blue (Stratagene, La Jolla, CA) was used as the host strain for all plasmid manipulations.

All *Acinetobacter* strains were cultured in Mueller-Hinton (MH) medium (broth or agar), supplemented with kanamycin (50 μg/ml) and carbenicillin (200 μg/ml) when appropriate. For biofilm studies, FAB medium [0.1 mM $CaCl_2$, 0.15 mM $(NH_4)_2SO_4$, 0.33 mM Na_2HPO_4, 0.5 mM NaCl, and 0.2 mM KH_2PO_4] supplemented with 10 mM sodium citrate and, unless otherwise indicated, 0.5% (wt/vol) Casamino Acids (FAB-citrate) was used. Static culture biofilm experiments for time course confocal microscopy were incubated at 37°C in room air on a heated microscope stage; in all other cases, bacteria were grown at 35.5°C in 5% CO_2.

Plasmid pMU125, an *E. coli-Acinetobacter* shuttle vector conferring green fluorescent protein (GFP) expression (14), was generously provided by Luis Actis.

DNA and RNA manipulations. Routine DNA manipulations were performed using standard procedures (37). Chromosomal DNA was purified as previously described (36). Restriction endonucleases were supplied by New England Biolabs, Inc. (Ipswich, MA), and Promega Corp. (Madison, WI); assays were performed as recommended by the manufacturer. Oligonucleotide primers were purchased from Integrated DNA Technologies (Coralville, IA).

Total RNA was isolated by using an RNeasy minikit (Qiagen, Santa Clara, CA), and transcriptional analysis was performed by using a OneStep reverse transcriptase-PCR (RT-PCR) kit (Qiagen) and the primers listed in Table 1.

MAb development. MAb 6E3, an immunoglobulin G1 isotype that reacts to an epitope on Bap, was developed by injecting BALB/c mice intraperitoneally with live *A. baumannii* 307-0294 suspended in phosphate-buffered saline according to a previously described protocol (5). Hybridoma supernatants were screened by immunodot and Western blot assays for the presence of antibody reactive to whole bacteria, whole-cell lysate, and proteinase K-digested whole-cell lysate of *A. baumannii* 307-0294.

Hybridoma cell line 6E3 produced antibody reactive to a proteinase K-sensitive epitope on a high-molecular-weight antigen. This cell line was used to generate high-titer mouse ascites fluid and protein A affinity-purified antibody at a stock concentration of 2.2 mg/ml (Rockland Immunochemicals, Gilbertsville, PA).

Transposon mutagenesis. EZ-Tn*5* Kan-2 Transposomes (Epicenter, Madison, WI) were electroporated into electrocompetent *A. baumannii* 307-0294, prepared by washing log-phase bacteria (optical density at 600 nm [OD_{600}] ≈ 1) three times with ice-cold sterile ultrapure water and resuspending them in ice-cold sterile 10% glycerol. Electrocompetent cells were stored in 50-μl single-use aliquots at −80°C. Transformants were selected with kanamycin and screened for surface reactivity to MAb 6E3 by colony lift assay.

Flow cytometry. Wild-type *A. baumannii* 307-0294 and *bap1302*::EZ-Tn*5* from late-log-phase growth (OD_{600} ≈ 1.8) in MH broth cultures were diluted in sterile saline to an OD_{600} of 0.03. MAb 6E3 was labeled with the Zenon Alexa Fluor 488 Mouse IgG1 kit (Invitrogen Corp., Carlsbad, CA) according to the manufacturer's protocol. Blocking antibody, supplied with the kit, was labeled separately as a control for nonspecific binding. A total of 1 μg of labeled antibody was added to 100 μl of diluted bacteria, followed by incubation at room temperature for 20 min. Then, 900 μl of sterile saline was added to the samples, and the cells were analyzed in a FACSCalibur flow cytometer (BD, Franklin Lakes, NJ) with the following settings: forward scatter voltage, E02 (log); side scatter voltage, 582 (log); FL1 voltage, 665 (log); event threshold, forward scatter = 434 and side scatter = 380.

DNA sequencing and computer analysis. The DNA sequence was determined by the dideoxy chain termination method using an ABI Prism 3130XL genetic analyzer (Applied Biosystems, Foster City, CA) at the Biopolymer Resource facility at Roswell Park Cancer Institute (Buffalo, NY). PCR products were cloned into the pGEM-T Easy vector (Promega), and genomic DNA was cloned into pUC18 after appropriate restriction endonuclease digestion. For sequencing the internal, highly repetitive region of *bap*, chromosomal DNA from nine transposon-insertion mutants, each with insertions in *bap*, was partially digested with Sau3AI, separated by 1.5% agarose gel electrophoresis to allow the selection of specific fragment sizes, and ligated into BamHI-digested pUC18. In some cases, nested deletions of the resultant plasmids were generated by using the Erase-a-Base system (Promega). The sequence of the genomic regions neighboring *bap* was determined by pyrophosphate-based sequencing by synthesis on a 454 Genome Sequencer 20 DNA sequencing system (Roche Applied Science, Indianapolis, IN) at the New York State Center of Excellence in Bioinformatics and Life Sciences (Buffalo, NY). Sequence similarity searches were performed by using the BLAST and BLASTP programs at the National Center for Biotechnology Information (NCBI). All other sequence assembly and analysis was performed by using the MacVector software package (v7.2.3; MacVector, Inc., Cary, NC).

SDS-PAGE, Western blotting, and colony lift immunoassay. Sodium dodecyl sulfate-polyacrylamide gel electrophoresis (SDS-PAGE), Western blotting, and colony lift analyses were performed according to standard procedures (37), with the exception that protein samples were not boiled prior to gel electrophoresis. Equal amounts of protein were loaded in each lane, and gels were stained with a Colloidal Blue staining kit (Invitrogen). Western blots and colony lift immunoassays were probed with MAb 6E3 and detected colorimetrically with horseradish peroxidase-conjugated secondary antibody (KPL, Inc., Gaithersburg, MD). Whole-cell protein extracts were prepared with a BugBuster protein extraction reagent (Novagen) according to the manufacturer's protocol. Zwittergent-extracted outer membrane proteins were prepared as described previously (6).

NanoLC-MS/MS. The protein identification work was performed by ProtTech, Inc. (Norristown, PA) using nanoscale liquid chromatography with tandem mass spectrometry (NanoLC-MS/MS) peptide sequencing technology. In brief, each protein gel band was destained, cleaned, and digested in-gel with sequencing-grade modified trypsin. The resultant peptide mixture was analyzed by an LC-MS/MS system, and the mass spectrometric data acquired were used to search the most recent nonredundant and patent protein databases with ProtTech's proprietary software suite.

Static culture biofilm growth for confocal microscopy. For single-time-point biofilm imaging, *A. baumannii* 307-0294 and *bap1302*::EZ-Tn*5* were resuspended from an overnight MH plate and inoculated into 35-mm glass-bottom petri dishes (MatTek, Corp., Ashland, MA). The plates were incubated at 35.5°C for 48 h and then stained with a LIVE/DEAD *Bac*Light bacterial viability kit (Invitrogen) according to the manufacturer's instructions. Image stacks were acquired by confocal laser scanning microscopy (CLSM) at ×630 magnification on a Zeiss Axiovert 200M inverted microscope with an attached Zeiss LSM 510 Meta NLO imaging system. Images were produced from the raw LSM files by using ImageJ (freely available from the National Institutes of Health).

For time course biofilm imaging, *A. baumannii* 307-0294 and *bap1302*::EZ-Tn*5* were transformed by electroporation with pMU125. The resultant GFP-express-

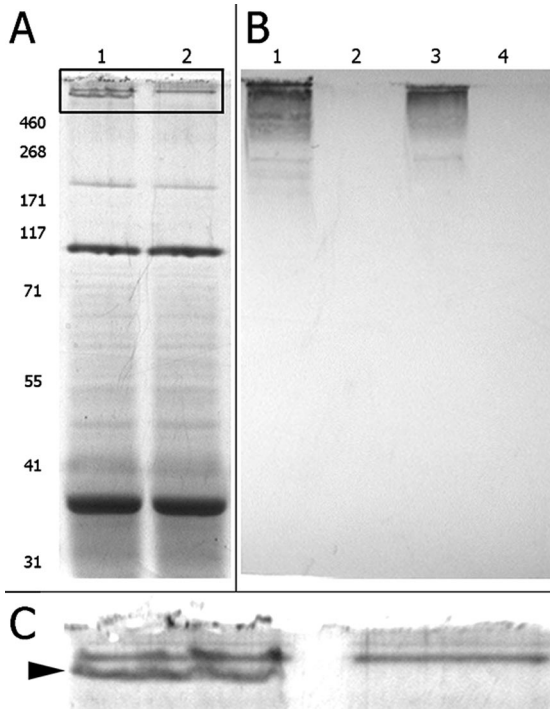

FIG. 1. Coomassie blue-stained SDS–7% polyacrylamide gel (A and C) and immunoblot (B) demonstrating reactivity of MAb 6E3 to a high-molecular-weight antigen in *A. baumannii* 307-0294 whole-cell lysate (lane 1) and outer membrane proteins (lane 3) but not the corresponding samples from *A. baumannii bap1302*::EZ-Tn*5* (lanes 2 and 4, respectively). (C) Enlargement of the region outlined in panel A to clearly show the high-molecular-weight antigen present in wild type and absent in *A. baumannii bap1302*::EZ-Tn*5* whole-cell lysate. This band was excised from a similar gel and identified by NanoLC-MS/MS. Molecular mass standards are indicated in kilodaltons.

ing strains were incubated overnight at 35.5°C on MH agar with appropriate antibiotics. Cells were resuspended in FAB-citrate to an OD_{600} of 0.4, and 10 μl was inoculated into four-well chambered coverglass slides (Nunc; Lab-Tek catalog no. 136420) containing 1 ml of FAB-citrate. The slides were loaded onto the motorized preheated stage of the CLSM system, and image stacks were acquired every 60 min for 14 h from two nonoverlapping fields of view at ×400 magnification, covering a total slide surface area of 10^5 μm^2, in order to obtain a representative sample of the biofilm (21). The CLSM image stacks were manually edited to remove extraneous images (defined as any image including and below those containing reflections of the glass coverslip and any images including and above the first image to contain no bright pixels representing bacterial cells) to minimize bias during quantitative image analysis (29). The manually edited image stacks were analyzed by using the Image Structure Analyzer-3D program to calculate 20 parameters describing the three-dimensional biofilm structure (2), including biovolume and average thickness at each time point for each field of view. Statistical analyses were performed with Prism (version 4.0c; GraphPad Software, Inc.) by fitting the data with the best-fit fourth-order polynomial equation and performing an F test of the null hypothesis that the curves describing biofilm development by wild-type and mutant bacteria were best described by the same equation. Inverse biofilm experiments using 96-well polystyrene plates were performed as described previously (28).

Nucleotide sequence accession number. The *A. baumannii* 307-0294 *bap* locus, with each repeat unit annotated, has been deposited in GenBank under accession number EU117203.

RESULTS

Characterization of MAb 6E3. Immunodot assay was initially used to identify MAb 6E3, which reacted to whole-cell lysates of *A. baumannii* 307-0294 (data not shown). Western blot analysis demonstrated that the MAb 6E3 epitope is detected on a high-molecular-weight antigen present in whole-cell lysate and outer membrane proteins of *A. baumannii* 307-0294 (Fig. 1B). The epitope is sensitive to proteinase K digestion, and the electrophoretic mobility of the antigen is modified by heat but not by SDS or β-mercaptoethanol (data not shown).

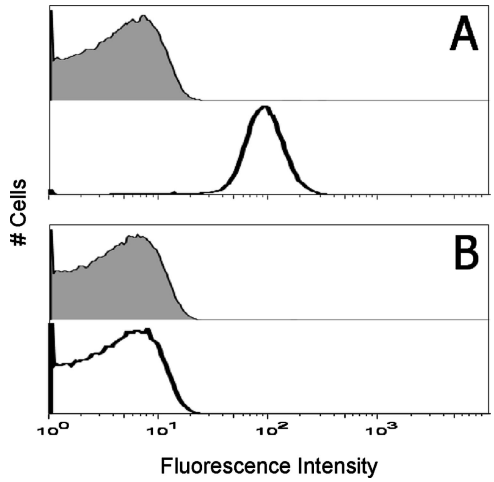

FIG. 2. Flow cytometric analysis of *A. baumannii* 307-0294 (A) and *bap1302*::EZ-Tn*5* (B) demonstrates the surface accessibility of the MAb 6E3 epitope. Cells from late-log-phase cultures were probed with Alexa Fluor 488-conjugated control nonspecific antibody (shaded histograms) or MAb 6E3 (unshaded histograms). Each histogram shows the fluorescence intensity distribution of >50,000 flow cytometer events.

The MAb 6E3 antigen contains surface-exposed epitopes. Flow cytometry was used to determine whether the antigen recognized by MAb 6E3 was surface accessible. Figure 2 shows that MAb 6E3 binds to an epitope expressed on the surface of wild-type *A. baumannii* 307-0294 (Fig. 2A), whereas the Bap-deficient mutant *bap1302*::EZ-Tn*5* (described below) has lost

TABLE 2. Survey of MAb 6E3 reactivity among a representative library of *Acinetobacter* strains isolated during an outbreak in the U.S. military health care system

Acinetobacter species	Sequence type[a]	No. of strains:		No. of strains reactive to MAb 6E3 (%)
		Isolated	Screened	
A. baumannii		189	76	31 (41)
	ST11	51	5	4 (80)
	ST14	22	6	6 (100)
	ST16	13	2	2 (100)
	ST10	12	2	2 (100)
	Other[b]	91	61	17 (28)
13TU		8	5	0 (0)
Genome sp. 3		13	13	11 (85)
Other[c]		6	4	0 (0)
Total		216	98	42 (43)

[a] Sequence type assignments were extracted from Fig. 2 in reference 15.
[b] Includes strains representing 35 other sequence types and two isolates of unknown sequence type.
[c] Includes one isolate of genome species 10 and three otherwise undescribed genomic species; additional single isolates of *A. ursingii* and *A. haemolyticus* were recovered during the outbreak, but these were not included in our screened library.

TABLE 3. Internal peptide fragments of Bap identified by NanoLC-MS/MS from a single band on a protein gel

Peptide mass (Da)	Peptide sequence	Position (start-end)
1,141.64	VAASDVLVVNR	35–45
2,630.35	NIPADAANTAVTVVINGVTYNATVDK	228–253
1,900.95	AAGTWTVSVPGSGLVADADK	254–273
2,596.33	TVVADSSDTGVIDLLGIFGSEVQFK	8032–8056
1,642.78	VDSFTYTVSDPVTGR	8181–8195
1,690.84	PLDSAANATVDVIDYK	8444–8459

reactivity to this antibody (Fig. 2B). These data confirm that the epitope on the high-molecular-weight antigen recognized by MAb 6E3 is surface exposed.

The MAb 6E3 epitope is conserved among recent clinical isolates. A panel of 98 *Acinetobacter* strains, representing the 216 isolates recovered during an outbreak in the U.S. military health care system (15), was screened by colony lift assay to determine the level of conservation of the MAb 6E3 epitope. The results of these studies demonstrate that 43% of *Acinetobacter* isolates are reactive to MAb 6E3 (Table 2).

Peptide sequence from the MAb 6E3 antigen. The high-molecular-weight protein band reactive to MAb 6E3 was excised from a Coomassie blue-stained SDS-polyacrylamide gel and identified by LC-MS/MS peptide sequencing. Six peptides were sequenced (Table 3), and the sequences were concatenated and subjected to BLASTP analysis against the patented protein sequence database at the NCBI, which identified sequence 5503 from U.S. patent 6562958 (entitled "Nucleic acid and amino acid sequences relating to *Acinetobacter baumannii* for diagnostics and therapeutics"). A similar search performed against the nonredundant protein sequence database identified a small number of repetitive surface proteins, as well as two predicted proteins from *A. baumannii* ATCC 17978: A1S_2724, a putative hemagglutinin/hemolysin-related protein, and A1S_2696, a hypothetical protein.

Random transposon mutagenesis. In order to identify the gene encoding the high-molecular-weight proteinaceous antigen described above, we screened 550 kanamycin-resistant EZ-Tn*5* insertional mutants and identified nine that lost surface reactivity to MAb 6E3. We obtained DNA sequence flanking the transposon insertion site for each of the nine mutants that suggested a common gene was disrupted.

The full-length coding sequence of the disrupted gene was assembled from sequence data obtained as described in Materials and Methods. BLASTP analysis against the nonredundant protein sequences database at the NCBI showed that this coding sequence was similar to Baps from various bacterial species. The predicted full-length *A. baumannii* 307-0294 *bap* open reading frame is 25,863 bp and composed primarily of four similar, tandem repeated modules (designated modules A to D), ranging in size from 237 to 315 bp (Fig. 3A). The 3′ end of the coding sequence contains additional repeat modules (designated modules E to G) that are not similar to modules A to D.

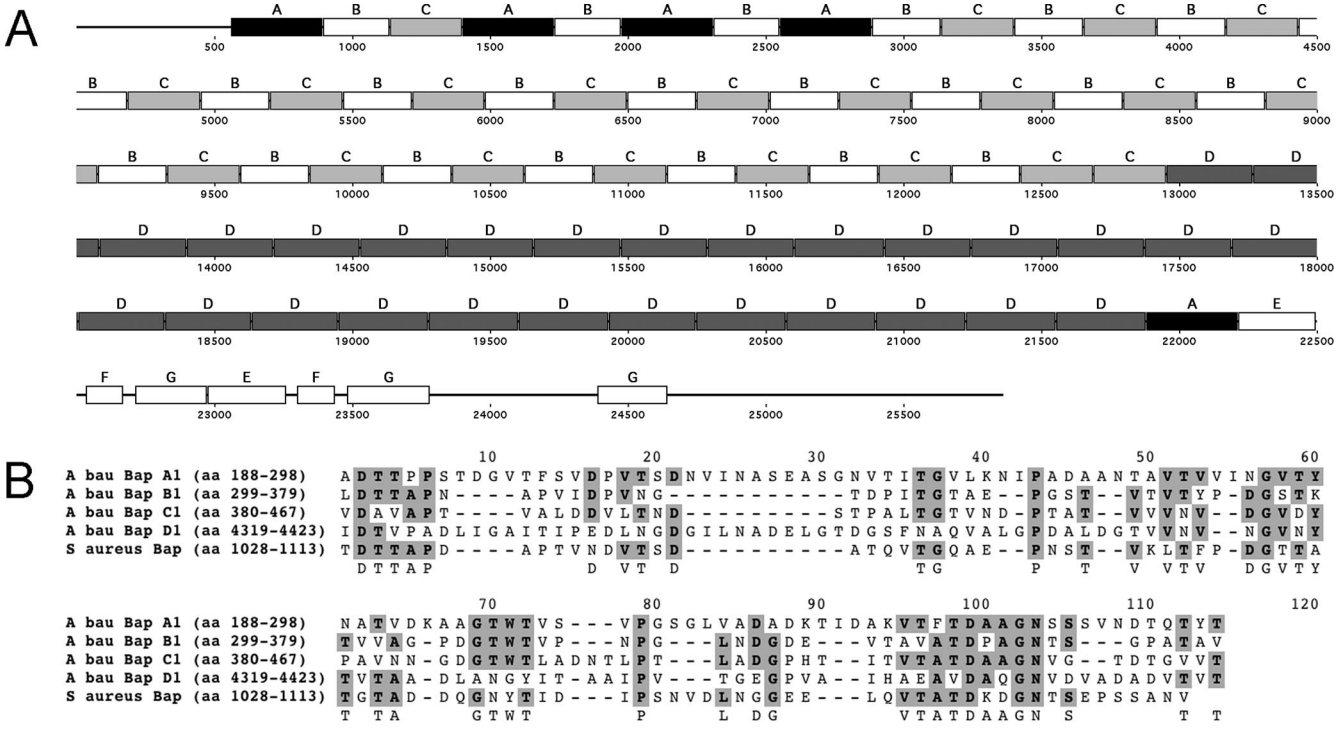

FIG. 3. Graphical representation of *bap* demonstrating the repetitive structure (A) and a CLUSTAL alignment (B) showing sequence similarity between the $Bap_{A.\ baumannii}$ and $Bap_{S.\ aureus}$ repeat units. (A) The 25,863-bp *A. baumannii bap* open reading frame is composed almost entirely of tandemly arranged repeats, labeled A to D. The 3′ end of the coding sequence contains additional repetitive units E to G that are not similar to A to D. (B) CLUSTAL alignment of an example of each of the major repeat types found in $Bap_{A.\ baumannii}$ and of the "C" repeat unit from $Bap_{S.\ aureus}$. For both proteins, the start and end of each repeat, indicated in parentheses, was defined by comparison to the seed alignment of the HYR domain (PFAM accession no. PF02494).

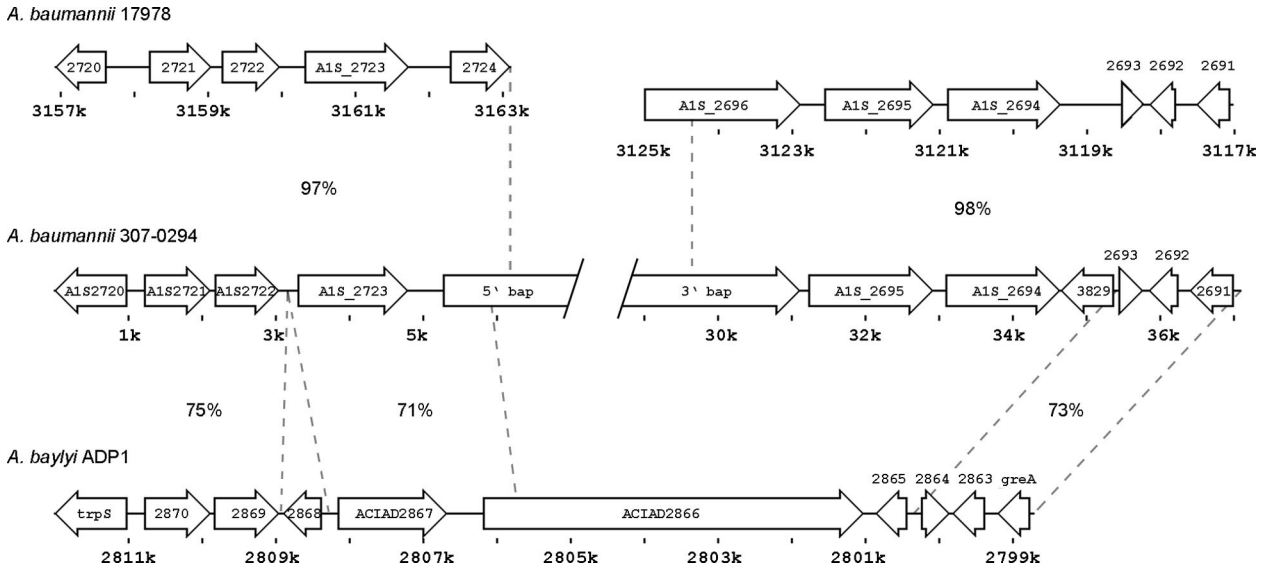

FIG. 4. The publicly available *Acinetobacter* genomes *A. baumannii* 17978 (NCBI accession no. NC_009085.1) and *A. baylyi ADP1* (NCBI accession no. NC_005966.1) contain regions homologous to the *bap* locus in *A. baumannii* 307-0294. The rulers indicate the size (*A. baumannii* 307-0294) and genomic coordinates (*A. baumannii* 17978 and *A. baylyi* ADP1) of the fragments. The percent nucleotide identity is shown for the regions delimited by dashed lines. Predicted open reading frames in *A. baumannii* 307-0294 are annotated with the identifier of the homologous open reading frame in *A. baumannii* 17978 (prefix A1S_, except for AS1_3829), and those in *A. baylyi* ADP1 are annotated with the gene symbol when available and the serially numbered identifiers (prefix ACIAD) otherwise. Note that the rulers for the two *A. baumannii* 17978 fragments are not continuous and not even in the same direction: the fragments in the assembled genome are in opposition relative to the arrangement in *A. baumannii* 307-0294 and *A. baylyi* ADP1 and are separated by over 30 kb of intervening genomic DNA that is not similar to *bap*.

Each of the peptides identified by nanoLC-MS/MS (Table 3) is found within the translated predicted *bap* open reading frame. As mentioned above, BLASTP analysis of the predicted amino acid sequence against the nonredundant protein database at the NCBI demonstrates regions of sequence similarity to the Baps from several staphylococcal species, including *S. hyicus* Bap (accession no. AAY28520.1), *S. aureus* Bap (accession no. AAK38834.2), and *S. epidermidis* Bap (accession no. AAY28519.1).

A. baumannii bap1302::EZ-Tn*5* was selected from the nine available *bap*-insertional mutants because it contains a transposon insertion closest to the predicted *bap* start codon, preventing translation of the 95% of the gene that is 3′ to the insertion site. Whole-cell lysates of wild-type *A. baumannii* 307-0294 and *bap1302*::EZ-Tn*5* were analyzed by SDS-PAGE (Fig. 1A), demonstrating that the wild type contained a high-molecular-weight band (Fig. 1C, lane 1) that was missing in the mutant (lane 2). In addition, Western blot analysis confirmed that whole-cell lysate and outer membrane proteins of *A. baumannii bap1302*::EZ-Tn*5* lost reactivity to MAb 6E3 (Fig. 1B, lanes 2 and 4).

Characterization of *bap* transcription by RT-PCR. *A. baumannii bap1302*::EZ-Tn*5* was further analyzed to determine whether the transposon insertion resulted in downstream polar effects. We performed RT-PCR to determine whether *bap* and A1S_2695 were cotranscribed (see Fig. 4 for the genetic arrangement of the *bap* locus in *A. baumannii* 307-0294). Oligonucleotide primers (Table 1) were designed to amplify regions of *bap* up- and downstream of the transposon insertion site; primers were also designed for an internal region of A1S_2695 and for a region spanning the intergenic region linking *bap* to A1S_2695. The results in Fig. 5 demonstrate that *bap* and A1S_2695 are not cotranscribed: therefore, disruption of *bap* does not appear to exert polar effects on neighboring genes.

Structural features of Bap. Bap is composed primarily of multiple copies of seven repeat units (designated A to G; see

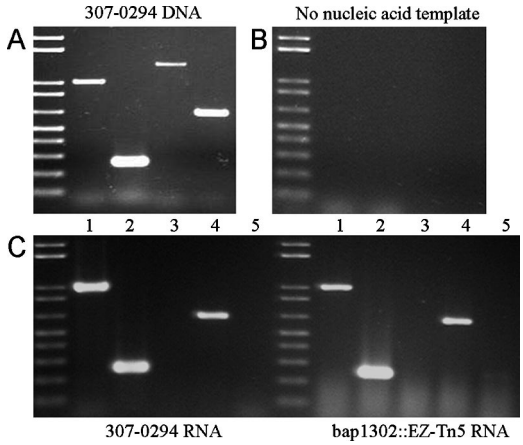

FIG. 5. RT-PCR and agarose gel electrophoresis demonstrates that *bap* and A1S_2695 are not cotranscribed and that transcription of A1S_2695 is not disrupted in *A. baumannii bap1302*::EZ-Tn*5*. (A) Each primer set amplifies a product from chromosomal DNA template. Pr1160-1330 (lane 3), however, fails to amplify a product from RNA template (C), indicating that *bap* and A1S_2695 are not present on the same fragment of RNA. The samples in lane 5 included RNA template but were not subject to the RT step, as a control for DNA contamination, and hence were not applicable to the reaction sets containing either chromosomal DNA (A) or no nucleic acid template (B). Primers (Table 1) were designed to target the indicated regions: lane 1, 5′ *bap*; lane 2, 3′ *bap*; lane 3, 3′ *bap*-A1S_2695; lane 4, A1S_2695; and lane 5, 3′ *bap* (no template control).

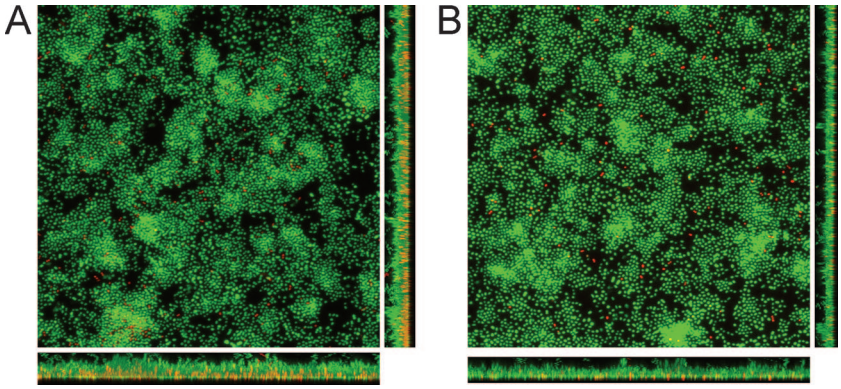

FIG. 6. CLSM images of biofilms formed by *A. baumannii* 307-0294 (A) and *bap1302*::EZ-Tn*5* (B) clearly demonstrate the decreased thickness achieved by the mutant after 48 h in static culture. Biofilms were grown in 35 mm glass-bottom petri dishes for 48 h and stained with the LIVE/DEAD *Bac*Light bacterial viability kit, which stains live cells green with SYTO-9 and dead cells red with propidium iodide. The images show the average intensity projections through the confocal image stack, with the maximum intensity *x-z* and *y-z* projections shown along the bottom and side of each image. Images were produced in ImageJ.

Fig. 3A); there are 5 copies of repeat module A (54 to 99% amino acid sequence identity between copies), 22 copies of module B (72 to 100%), 21 copies of module C (73 to 100%), 28 copies of module D (78 to 100%), 2 copies of module E (62%), 2 copies of module F (67%), and 3 copies of module G (36 to 51%). For the majority of the sequence (amino acids 188 to 7499, out of 8,621), the repeat modules are directly in tandem, with no additional amino acids between consecutive repeats.

Analysis of the primary structure reveals the absence of Cys and an abundance of Thr (1,389 residues; 16% of the total), Ala (1,176 residues; 14% of the total), and Val (1,109 residues; 13% of the total). In addition, Bap has a remarkably low isoelectric point (pI), estimated to be 2.9, placing it among the most acidic bacterial proteins thus far described. The low pI may explain why the presence of SDS during electrophoresis has no apparent effect (data not shown), since very acidic proteins do not bind SDS under standard SDS-PAGE conditions (18), and is a reflection of an 11:1 imbalance in the number of acidic and basic amino acids: there are 1,168 acidic (984 Asp + 184 Glu) and 105 basic residues (60 His + 34 Lys + 11 Arg). Since trypsin cleaves exclusively after Lys and Arg (33), the paucity of these amino acids explains why only a few peptides were sequenced after tryptic digestion of Bap (Table 3).

BLASTP analysis of the "D" repeat region, which in aggregate contains 35% of the total amino acids, identifies similarities to a putative outer membrane adhesin from *Shewanella* sp. strain ANA-3 (accession number YP_868031), whereas the similarity to the staphylococcal Baps is limited to the "A-C" repeats, which contain 48% of the total amino acids. CLUSTAL alignment of repeat units A to D from $Bap_{A.\ baumannii}$ and C from $Bap_{S.\ aureus}$ (Fig. 3B) indicated that sequence similarities are limited to small stretches of amino acids (particularly in positions 2 to 6 [consensus DTTAP] and 95 to 103 [consensus VTATDAAGN]), which are separated from each other by longer stretches with more divergent sequence.

Comparison of the *bap* locus in *A. baumannii* 307-0294 with homologous loci in other *Acinetobacter* species. There are two publicly available *Acinetobacter* genomes: *A. baylyi* ADP1 and *A. baumannii* 17978, and we have identified regions homologous to the *A. baumannii* 307-0294 *bap* locus in each (Fig. 4). *A. baumannii* 307-0294 *bap* is flanked by *nhaP* (A1S_2723) upstream, and a putative glucosyltransferase (A1S_2695) downstream, with all three genes in the same orientation. *A. baylyi* ADP1 contains a single contiguous genomic region with a 5-kb putative hemagglutinin in place of the 26-kb *bap* open reading frame. The published genome for *A. baumannii* 17978 (40), surprisingly, does not contain a single homologous locus but rather two loci separated by 30 kb of unrelated sequence and oriented in opposition relative to the organization in *A. baylyi* ADP1 and *A. baumannii* 307-0294. The nonrepetitive 5′ and 3′ ends of *bap* are annotated as two distinct putative open reading frames in *A. baumannii* 17978, and the internal repeats are not found in the assembled genome. *A. baumannii* 17978 and *A. baylyi* ADP1 are not reactive to MAb 6E3 (data not shown).

Disruption of *bap* diminishes biovolume and biofilm thickness. Biofilms formed by *A. baumannii* 307-0294 and *bap1302*::EZ-Tn*5* after 48 h of static culture in FAB-citrate supplemented with 0.05% (wt/vol) Casamino Acids were stained with a LIVE/DEAD stain and imaged by CLSM (Fig. 6). Upon examination of these confocal micrographs, the biofilm formed by wild-type bacteria was noticeably thicker than that formed by mutant bacteria. In order to more carefully analyze this difference, we designed an experiment that allowed us to quantify the dynamics of biofilm development over time.

Static cultures of GFP-expressing *A. baumannii* 307-0294 and *bap1302*::EZ-Tn*5* were imaged every hour for 14 h to visualize and quantify biofilm development on glass coverslips. The resultant image stacks were analyzed by using the ISA-3D software program (2) and, of the 20 calculated parameters, 2 followed significantly different trends over time for the mutant compared to wild-type biofilms: mean biofilm thickness and total biovolume (Fig. 7). Specifically, biofilms formed by wild-type and mutant bacteria are distinguishable after 6 h, when the mutant reaches a biofilm thickness plateau that is less than half that ultimately achieved by wild-type bacteria. The mutant also steadily loses biovolume for the remainder of the experiment, in contrast to the stable biovolume maintained by wild-

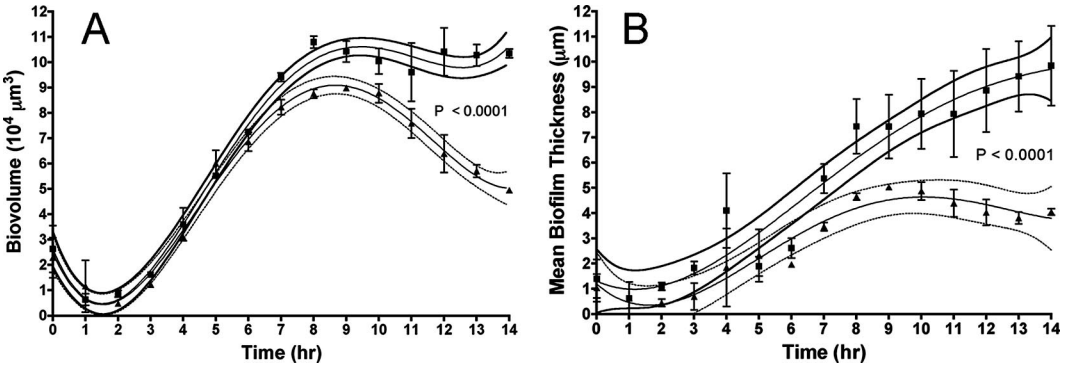

FIG. 7. Comparison of biovolume (A) and mean biofilm thickness (B) achieved by *A. baumannii* 307-0294 (■) and *A. baumannii bap1302*::EZ-Tn*5* (▲) during static culture. The data points are the means ± the standard deviations for two separate high-power fields of view, representing a total slide surface area of 10^5 μm^2 per sample. The best-fit nonlinear regression curve is shown as a thin trend line with 95% confidence bands. Because the biofilms formed by wild-type and mutant bacteria cannot be described with the same curve ($P < 0.0001$), we conclude that the biofilms differ significantly with respect to biovolume and mean biofilm thickness development over time.

type bacteria. It is important to note that these differences are specific to biofilm formation, since these strains are indistinguishable by growth curve analysis in shaking broth cultures in the same FAB-citrate media used in the static culture biofilm experiments (data not shown).

Semiquantitative analysis of biofilms grown on polystyrene pins in 96-well plates is consistent with the results obtained from the confocal experiments: the biofilm formed by the *bap1302*::EZ-Tn*5* retains less crystal violet stain, indicative of less accumulated biovolume, compared to the wild type (data not shown).

DISCUSSION

A. baumannii is an opportunistic pathogen that is particularly successful at colonizing and persisting in the hospital environment, able to resist desiccation (19, 20, 53) and survive on inanimate surfaces for months (22). It is among the most common causes of device-related nosocomial infection (13, 43, 52), which result when the organism is able to resist physical and chemical disinfection, often by forming a biofilm (7, 27, 34). We chose to study biofilm formation by *A. baumannii* in order to understand how this pathogen persists in the hospital environment to cause outbreaks worldwide (51).

Baps were first characterized in *S. aureus* (11) and have since been identified in a number of other gram-positive and gram–negative pathogenic bacteria (reviewed in references 24 and 25). They are defined by shared structural and functional characteristics and are essentially high-molecular-weight, repetitive surface proteins involved in biofilm formation (24). The prototypical Bap from *S. aureus* is involved in the primary attachment step of biofilm formation, as well as in promoting intercellular adhesion and biofilm maturation (11); other Baps are involved in the various stages of biofilm formation and in adhesion to eukaryotic host cells (25).

We have identified a protein produced by *A. baumannii* 307-0294 that satisfies all of the criteria to be included in the Bap family: it is high molecular weight, with a predicted molecular mass of 854 kDa; it is repetitive, composed of multiple copies of seven repeat modules (A to G); it is exposed on the surface; and it is involved in biofilm formation and development.

There are several conceptual, sequential stages in bacterial biofilm formation (reviewed in reference 41): (i) reversible primary attachment of individual cells to a surface, (ii) progression to irreversible attachment mediated by extracellular polysaccharide, (iii) early development of biofilm architecture, (iv) maturation of biofilm architecture, and (v) dispersal of single cells from the biofilm. Bap$_{A.\ baumannii}$ does not appear to be involved in the primary attachment of cells to glass or polystyrene, in contrast to Bap$_{S.\ aureus}$ (11). Our data suggest that Bap$_{A.\ baumannii}$ appears to be involved in maintaining the mature biofilm architecture (steps 3 and 4), since biofilms formed by the mutant are neither as thick nor as voluminous as those formed by the wild type. There are at least three potential Bap-mediated interactions to explore in future studies: (i) Bap$_{A.\ baumannii}$ may mediate direct intercellular adhesion from one bacterium to a surface receptor on a neighboring bacterium, (ii) this may be an example of autoadhesion between Bap molecules on adjacent bacteria, or (iii) cells may be linked indirectly via shared interactions with some extracellular biofilm matrix component. While these are all logical hypotheses, further studies are needed in order to carefully determine the actual function of Bap$_{A.\ baumannii}$.

Bap is a remarkable protein: it contains 8,621 amino acids, making it one of the largest bacterial proteins yet described; it has a predicted pI of 2.9, making it one of the most acidic bacterial proteins; and it is composed of tandemly arranged repeat modules. The protein is divided almost equally in two parts: the first contains modules A to C, alternating one after the other; the second contains 28 direct tandem repeats of module D. Each repeat unit A-D appears to be related to the HYR domain (4) (PFAM accession no. PF02494) based on the conserved amino acids DTTAP and VTATDAAGN (Fig. 3), although the HYR seed alignment contains two conserved cysteines that are conspicuously absent from Bap. HYR was first identified in eukaryotic proteins involved in cellular adhesion and is found in a number of large repetitive prokaryotic proteins as well, including several adhesins (4). Three-dimensional structure prediction using the PHYRE server (http:

//www.sbg.bio.ic.ac.uk/phyre/) suggests that each module A-D folds into a seven-stranded β-sandwich similar to proteins within the immunoglobulin-like fold superfamily (PFAM accession no. CL0159, which includes the HYR domain as a family member). This suggests Bap adopts a "beaded-filament" tertiary structure and that each module might redundantly contribute to the overall function. Other bacterial proteins that adopt a tertiary structure similar to that predicted for Bap include invasin from *Yersinia pseudotuberculosis* and intimin, FimH, and PapG from enteropathogenic *E. coli* (32). The latter two proteins are actually individual subunits that resemble an isolated repeat unit of Bap and are assembled into filamentous pili that recapitulate in quaternary structure what Bap is predicted to accomplish in tertiary structure. The pattern of sequence similarity to $Bap_{S.\ aureus}$ (Fig. 3B), with short stretches of highly conserved residues separated by longer regions of divergence, suggests that the conserved regions might function to maintain a common structural motif, while the divergent regions might confer unique functionality to the respective proteins. In this light, it is interesting that $Bap_{A.\ baumannii}$ contains four distinct modules (A to D), each based on the same HYR motif, whereas $Bap_{S.\ aureus}$ seems to contain multiple copies of only a single repeat type.

Using a previously reported typing scheme (15), *A. baumannii* 307-0294 is a sequence type ST15 (data not shown). ST15 is phylogenetically linked with European hospital clone I (15, 35), which is associated with epidemic behavior and multidrug resistance (31, 35, 47). Although at least 39 sequence types of *A. baumannii* were distinguished among the military outbreak strains (15), four of them (ST11, ST14, ST16, and ST10) accounted for over half of the isolates, suggesting either that the outbreak was clonal in nature or that particular sequence types of *A. baumannii* are more likely to cause human infection. It is intriguing that MAb 6E3 recognizes 14 of 15 (93%) of the representatives from these four sequence types compared to 17 of 61 (28%) of the representatives from the other 35 sequence types (Table 2), although the significance of this observation is not clear. For example, we do not know whether the strains that failed to react to MAb 6E3 did not express a Bap homologue, or whether they expressed a variant that simply lacked the recognized epitope. For these reasons, and because we do not have access to disease severity information for the patients involved in the military outbreak, we are unfortunately unable to comment on the contribution of Bap to disease severity. Nevertheless, MAb 6E3 will be a useful tool for future studies designed to answer such questions.

In conclusion, we have identified a novel *A. baumannii* protein, Bap, expressed on the surface of these bacteria that is involved in biofilm formation in static culture. Bap has a predicted structure similar to bacterial adhesins within the immunoglobulin-like fold superfamily and may function as an intercellular adhesin in such a way that supports the mature biofilm structure. Although more studies are needed to test this hypothesis, a better understanding of the contribution of this Bap to *A. baumannii* biofilm formation and maturation may help to explain why *Acinetobacter* remains a common cause of nosocomially acquired device-related infection.

ACKNOWLEDGMENTS

David Craft and Paul Scott and the Walter Reed Army Medical Center generously provided a panel of 98 *Acinetobacter* strains recently isolated from infected military personnel serving in Iraq and Afghanistan (15). Thomas Russo provided *A. baumannii* 307-0294, originally isolated from the bloodstream of a patient in 1994. Luis Actis provided plasmid pMU125, an *E. coli-Acinetobacter* shuttle plasmid able to confer GFP expression in *Acinetobacter*. Haluk Beyenal generously provided the Image Structure Analyzer-3D software program, and Wade Sigurdson acquired the confocal microscopy images. Steven Gill provided a helpful critique of the manuscript.

Funding for this study was provided by U.S. Army Medical Research Acquisition Activity under contract W81XWH-05-1-0627.

REFERENCES

1. **Bergogne-Berezin, E., and K. J. Towner.** 1996. *Acinetobacter* spp. as nosocomial pathogens: microbiological, clinical, and epidemiological features. Clin. Microbiol. Rev. **9:**148–165.
2. **Beyenal, H., C. Donovan, Z. Lewandowski, and G. Harkin.** 2004. Three-dimensional biofilm structure quantification. J. Microbiol. Methods **59:**395–413.
3. **Bonomo, R. A., and D. Szabo.** 2006. Mechanisms of multidrug resistance in *Acinetobacter* species and *Pseudomonas aeruginosa*. Clin. Infect. Dis. **43**(Suppl. 2)**:**S49–S56.
4. **Callebaut, I., D. Gilges, I. Vigon, and J. P. Mornon.** 2000. HYR, an extracellular module involved in cellular adhesion and related to the immunoglobulin-like fold. Protein Sci. **9:**1382–1390.
5. **Campagnari, A. A., T. F. Ducey, and C. A. Rebmann.** 1996. Outer membrane protein B1, an iron-repressible protein conserved in the outer membrane of *Moraxella* (*Branhamella*) *catarrhalis*, binds human transferrin. Infect. Immun. **64:**3920–3924.
6. **Campagnari, A. A., K. L. Shanks, and D. W. Dyer.** 1994. Growth of *Moraxella catarrhalis* with human transferrin and lactoferrin: expression of iron-repressible proteins without siderophore production. Infect. Immun. **62:**4909–4914.
7. **Cappelli, G., L. Sereni, M. G. Scialoja, M. Morselli, S. Perrone, A. Ciuffreda, M. Bellesia, P. Inguaggiato, A. Albertazzi, and C. Tetta.** 2003. Effects of biofilm formation on haemodialysis monitor disinfection. Nephrol. Dial. Transplant. **18:**2105–2111.
8. **Chang, H. C., Y. F. Wei, L. Dijkshoorn, M. Vaneechoutte, C. T. Tang, and T. C. Chang.** 2005. Species-level identification of isolates of the *Acinetobacter calcoaceticus-Acinetobacter baumannii* complex by sequence analysis of the 16S-23S rRNA gene spacer region. J. Clin. Microbiol. **43:**1632–1639.
9. **Choi, C. H., E. Y. Lee, Y. C. Lee, T. I. Park, H. J. Kim, S. H. Hyun, S. A. Kim, S. K. Lee, and J. C. Lee.** 2005. Outer membrane protein 38 of *Acinetobacter baumannii* localizes to the mitochondria and induces apoptosis of epithelial cells. Cell Microbiol. **7:**1127–1138.
10. **Costerton, J. W., P. S. Stewart, and E. P. Greenberg.** 1999. Bacterial biofilms: a common cause of persistent infections. Science **284:**1318–1322.
11. **Cucarella, C., C. Solano, J. Valle, B. Amorena, I. Lasa, and J. R. Penades.** 2001. Bap, a *Staphylococcus aureus* surface protein involved in biofilm formation. J. Bacteriol. **183:**2888–2896.
12. **Davis, K. A., K. A. Moran, C. K. McAllister, and P. J. Gray.** 2005. Multidrug-resistant *Acinetobacter* extremity infections in soldiers. Emerg. Infect. Dis. **11:**1218–1224.
13. **Dima, S., E. I. Kritsotakis, M. Roumbelaki, S. Metalidis, A. Karabinis, N. Maguina, F. Klouva, S. Levidiotou, E. Zakynthinos, J. Kioumis, and A. Gikas.** 2007. Device-associated nosocomial infection rates in intensive care units in Greece. Infect. Control Hosp. Epidemiol. **28:**602–605.
14. **Dorsey, C. W., A. P. Tomaras, and L. A. Actis.** 2002. Genetic and phenotypic analysis of *Acinetobacter baumannii* insertion derivatives generated with a transposome system. Appl. Environ. Microbiol. **68:**6353–6360.
15. **Ecker, J. A., C. Massire, T. A. Hall, R. Ranken, T. T. Pennella, C. Agasino Ivy, L. B. Blyn, S. A. Hofstadler, T. P. Endy, P. T. Scott, L. Lindler, T. Hamilton, C. Gaddy, K. Snow, M. Pe, J. Fishbain, D. Craft, G. Deye, S. Riddell, E. Milstrey, B. Petruccelli, S. Brisse, V. Harpin, A. Schink, D. J. Ecker, R. Sampath, and M. W. Eshoo.** 2006. Identification of *Acinetobacter* species and genotyping of *Acinetobacter baumannii* by multilocus PCR and mass spectrometry. J. Clin. Microbiol. **44:**2921–2932.
16. **Falagas, M. E., I. A. Bliziotis, and I. I. Siempos.** 2006. Attributable mortality of *Acinetobacter baumannii* infections in critically ill patients: a systematic review of matched cohort and case-control studies. Crit. Care **10:**R48.
17. **Falagas, M. E., and E. A. Karveli.** 2007. The changing global epidemiology of *Acinetobacter baumannii* infections: a development with major public health implications. Clin. Microbiol. Infect. **13:**117–119.
18. **Garcia-Ortega, L., V. De los Rios, A. Martinez-Ruiz, M. Onaderra, J. Lacadena, A. Martinez del Pozo, and J. G. Gavilanes.** 2005. Anomalous electrophoretic behavior of a very acidic protein: ribonuclease U2. Electrophoresis **26:**3407–3413.
19. **Jawad, A., J. Heritage, A. M. Snelling, D. M. Gascoyne-Binzi, and P. M.**

Hawkey. 1996. Influence of relative humidity and suspending menstrua on survival of *Acinetobacter* spp. on dry surfaces. J. Clin. Microbiol. **34:**2881–2887.
20. **Jawad, A., H. Seifert, A. M. Snelling, J. Heritage, and P. M. Hawkey.** 1998. Survival of *Acinetobacter baumannii* on dry surfaces: comparison of outbreak and sporadic isolates. J. Clin. Microbiol. **36:**1938–1941.
21. **Korber, D. R., J. R. Lawrence, M. J. Hendry, and D. E. Caldwell.** 1993. Analysis of spatial variability within Mot^+ and Mot^- *Pseudomonas fluorescens* biofilms using representative elements. Biofouling **20:**334–358.
22. **Kramer, A., I. Schwebke, and G. Kampf.** 2006. How long do nosocomial pathogens persist on inanimate surfaces? A systematic review. BMC Infect. Dis. **6:**130.
23. **Lasa, I.** 2006. Towards the identification of the common features of bacterial biofilm development. Int. Microbiol. **9:**21–28.
24. **Lasa, I., and J. R. Penades.** 2006. Bap: a family of surface proteins involved in biofilm formation. Res. Microbiol. **157:**99–107.
25. **Latasa, C., C. Solano, J. R. Penades, and I. Lasa.** 2006. Biofilm-associated proteins. C. R. Biol. **329:**849–857.
26. **Lee, J. S., J. C. Lee, C. M. Lee, I. D. Jung, Y. I. Jeong, E. Y. Seong, H. Y. Chung, and Y. M. Park.** 2007. Outer membrane protein A of *Acinetobacter baumannii* induces differentiation of $CD4^+$ T cells toward a Th1 polarizing phenotype through the activation of dendritic cells. Biochem. Pharmacol. **74:**86–97.
27. **Loukili, N. H., B. Granbastien, K. Faure, B. Guery, and G. Beaucaire.** 2006. Effect of different stabilized preparations of peracetic acid on biofilm. J. Hosp. Infect. **63:**70–72.
28. **Mampel, J., T. Spirig, S. S. Weber, J. A. Haagensen, S. Molin, and H. Hilbi.** 2006. Planktonic replication is essential for biofilm formation by Legionella pneumophila in a complex medium under static and dynamic flow conditions. Appl. Environ. Microbiol. **72:**2885–2895.
29. **Merod, R. T., J. E. Warren, H. McCaslin, and S. Wuertz.** 2007. Toward automated analysis of biofilm architecture: bias caused by extraneous confocal laser scanning microscopy images. Appl. Environ. Microbiol. **73:**4922–4930.
30. **Navon-Venezia, S., A. Leavitt, and Y. Carmeli.** 2007. High tigecycline resistance in multidrug-resistant *Acinetobacter baumannii*. J. Antimicrob. Chemother. **59:**772–774.
31. **Nemec, A., L. Dijkshoorn, and T. J. van der Reijden.** 2004. Long-term predominance of two pan-European clones among multi-resistant *Acinetobacter baumannii* strains in the Czech Republic. J. Med. Microbiol. **53:**147–153.
32. **Niemann, H. H., W. D. Schubert, and D. W. Heinz.** 2004. Adhesins and invasins of pathogenic bacteria: a structural view. Microbes Infect. **6:**101–112.
33. **Olsen, J. V., S. E. Ong, and M. Mann.** 2004. Trypsin cleaves exclusively C-terminal to arginine and lysine residues. Mol. Cell Proteomics **3:**608–614.
34. **Pajkos, A., K. Vickery, and Y. Cossart.** 2004. Is biofilm accumulation on endoscope tubing a contributor to the failure of cleaning and decontamination? J. Hosp. Infect. **58:**224–229.
35. **Pantophlet, R., A. Nemec, L. Brade, H. Brade, and L. Dijkshoorn.** 2001. O-antigen diversity among *Acinetobacter baumannii* strains from the Czech Republic and Northwestern Europe, as determined by lipopolysaccharide-specific monoclonal antibodies. J. Clin. Microbiol. **39:**2576–2580.
36. **Russo, T. A., J. E. Guenther, S. Wenderoth, and M. M. Frank.** 1993. Generation of isogenic K54 capsule-deficient *Escherichia coli* strains through TnphoA-mediated gene disruption. Mol. Microbiol. **9:**357–364.
37. **Sambrook, J., and D. W. Russell.** 2001. Molecular cloning: a laboratory manual, 3rd ed. Cold Spring Harbor Laboratory Press, Cold Spring Harbor, NY.
38. **Scott, P. T., K. Petersen, J. Fishbain, D. W. Craft, A. J. Ewell, K. Moran, D. C. Hack, G. A. Deye, S. Riddell, G. Christopher, J. D. Mancuso, B. P. Petrucelli, T. Endy, L. Lindler, K. Davis, E. G. Milstrey, L. Brosch, J. Pool, C. L. Blankenship, C. J. Witt, J. L. Malone, D. N. Tornberg, A. Srinivasan, et al.** 2004. *Acinetobacter baumannii* infections among patients at military medical facilities treating injured U.S. service members, 2002–2004. Morb. Mortal. Wkly. Rep. **53:**1063–1066.
39. **Smith, M. G., S. G. Des Etages, and M. Snyder.** 2004. Microbial synergy via an ethanol-triggered pathway. Mol. Cell. Biol. **24:**3874–3884.
40. **Smith, M. G., T. A. Gianoulis, S. Pukatzki, J. J. Mekalanos, L. N. Ornston, M. Gerstein, and M. Snyder.** 2007. New insights into *Acinetobacter baumannii* pathogenesis revealed by high-density pyrosequencing and transposon mutagenesis. Genes Dev. **21:**601–614.
41. **Stoodley, P., K. Sauer, D. G. Davies, and J. W. Costerton.** 2002. Biofilms as complex differentiated communities. Annu. Rev. Microbiol. **56:**187–209.
42. **Talbot, G. H., J. Bradley, J. E. Edwards, Jr., D. Gilbert, M. Scheld, and J. G. Bartlett.** 2006. Bad bugs need drugs: an update on the development pipeline from the Antimicrobial Availability Task Force of the Infectious Diseases Society of America. Clin. Infect. Dis. **42:**657–668.
43. **Thongpiyapoom, S., M. N. Narong, N. Suwalak, S. Jamulitrat, P. Intaraksa, J. Boonrat, N. Kasatpibal, and A. Unahalekhaka.** 2004. Device-associated infections and patterns of antimicrobial resistance in a medical-surgical intensive care unit in a university hospital in Thailand. J. Med. Assoc. Thai. **87:**819–824.
44. **Tomaras, A. P., C. W. Dorsey, R. E. Edelmann, and L. A. Actis.** 2003. Attachment to and biofilm formation on abiotic surfaces by *Acinetobacter baumannii*: involvement of a novel chaperone-usher pili assembly system. Microbiology **149:**3473–3484.
45. **Tsakris, A., A. Ikonomidis, S. Pournaras, N. Spanakis, and A. Markogiannakis.** 2006. Carriage of OXA-58 but not of OXA-51 beta-lactamase gene correlates with carbapenem resistance in *Acinetobacter baumannii*. J. Antimicrob. Chemother. **58:**1097–1099.
46. **van den Broek, P. J., J. Arends, A. T. Bernards, E. De Brauwer, E. M. Mascini, T. J. van der Reijden, L. Spanjaard, E. A. Thewessen, A. van der Zee, J. H. van Zeijl, and L. Dijkshoorn.** 2006. Epidemiology of multiple *Acinetobacter* outbreaks in The Netherlands during the period 1999–2001. Clin. Microbiol. Infect. **12:**837–843.
47. **van Dessel, H., L. Dijkshoorn, T. van der Reijden, N. Bakker, A. Paauw, P. van den Broek, J. Verhoef, and S. Brisse.** 2004. Identification of a new geographically widespread multiresistant *Acinetobacter baumannii* clone from European hospitals. Res. Microbiol. **155:**105–112.
48. **Vidal, R., M. Dominguez, H. Urrutia, H. Bello, A. Garcia, G. Gonzalez, and R. Zemelman.** 1997. Effect of imipenem and sulbactam on sessile cells of *Acinetobacter baumannii* growing in biofilm. Microbios **91:**79–87.
49. **Vidal, R., M. Dominguez, H. Urrutia, H. Bello, G. Gonzalez, A. Garcia, and R. Zemelman.** 1996. Biofilm formation by *Acinetobacter baumannii*. Microbios **86:**49–58.
50. **Vila, J., S. Marti, and J. Sanchez-Cespedes.** 2007. Porins, efflux pumps, and multidrug resistance in *Acinetobacter baumannii*. J. Antimicrob. Chemother. **59:**1210–1215.
51. **Villegas, M. V., and A. I. Hartstein.** 2003. *Acinetobacter* outbreaks, 1977–2000. Infect. Control Hosp. Epidemiol. **24:**284–295.
52. **Wang, S. S., N. K. Chou, R. B. Hsu, W. J. Ko, H. Y. Yu, Y. S. Chen, S. C. Huang, N. H. Chi, C. S. Liau, and Y. T. Lee.** 2004. Heart transplantation in the patient under ventricular assist complicated with device-related infection. Transplant Proc. **36:**2377–2379.
53. **Wendt, C., B. Dietze, E. Dietz, and H. Ruden.** 1997. Survival of *Acinetobacter baumannii* on dry surfaces. J. Clin. Microbiol. **35:**1394–1397.